

Properties and Reactivity of Nanostructured CeO₂ Powders: Comparison among Two Synthesis Procedures

Marta M. Natile,* Giovanni Boccaletti, and Antonella Glisenti

Dipartimento di Scienze Chimiche, Università di Padova, via F. Marzolo, 1-35131 Padova, Italy

Received June 23, 2005. Revised Manuscript Received October 6, 2005

Three nanostructured cerium(IV) oxide powders were synthesized by two different synthetic routes: two samples were obtained by precipitation from a basic solution of cerium nitrate and treated at 523 and 923 K, respectively, and the third one was prepared by a microwave-assisted heating hydrolysis method and treated at 523 K. The obtained samples were characterized by means of X-ray diffraction (XRD), transmission electron microscopy (TEM), X-ray photoelectron (XPS), and diffuse reflectance infrared Fourier transform (DRIFT) spectroscopic techniques, thermal analysis, and Brunauer–Emmett–Teller (BET) surface area. A broad particle size distribution is observed for CeO₂ obtained by precipitation (8.0–15.0 nm). Smaller particles (sizes around 3.3–4.0 nm) with a narrow particle size distribution characterize the ceria obtained by microwave irradiation. XPS and DRIFT outcomes show that (i) the CeO₂ prepared by microwave-assisted heating hydrolysis method is more reduced than that obtained by precipitation and treated at the same temperature; (ii) the CeO₂ obtained by precipitation and treated at 923 K is more reduced than that prepared by microwave irradiation. A higher amount of basic and acidic sites were noticed on the CeO₂ obtained by microwave irradiation. Methanol interacts mainly dissociatively with the CeO₂ surface regardless of the preparation procedure and reduction degree of surface; however, on the CeO₂ prepared by microwave irradiation the interaction is quantitative: all the methanol introduced in the reaction chamber reacts with the surface. The CeO₂ obtained by precipitation and treated at 523 K does not oxidize methanol, even at higher temperature, while traces of oxidation products are noted on the sample treated at 923 K. Methanol oxidation is favored on the CeO₂ prepared by microwave irradiation: the main oxidation products are formate species and inorganic carboxylate. Moreover, the oxidation capability increases with increasing temperature.

Introduction

In recent years cerium oxide has been attracting great interest because of the effective and the potential technological applications in several fields such as catalysis, electrochemistry, photochemistry, and materials science. It is a highly refractory oxide and possesses a fluorite-type crystal structure in which each metal cation is surrounded by eight oxygen atoms. The oxygen storage capacity (OSC) associated with the ability to undergo a facile conversion between Ce(IV) and Ce(III) is one of its most interesting properties.¹ Ceria is a key component in three-way catalysts (TWC)¹ and is used as a base material for electrolytes and electrodes in solid oxide fuel cells (SOFCs).²

Nanostructured CeO₂ can impact significantly in all these practical applications due to the general improvement in its physical and chemical properties (thermal stability and redox properties are an example) with respect to bulklike materials. Nanocrystals in the 1–10 nm range, in fact, display properties significantly different from those of their microcrystalline counterparts. The main difference in the properties of nanocrystalline materials compared to bulk materials is attributed to the enhanced surface area (due to the higher

fraction of atoms lying on or near the surface). In addition, the more polyhedral shapes and the high density of surface active sites of nanostructured materials also favor improved performances with respect to the conventional materials.³

During these years several synthetic procedures have been developed to produce nanocrystalline CeO₂ powders including hydrothermal synthesis,^{4–6} homogeneous precipitation with urea or hexamethylenetetramine,^{7,8} flame spray pyrolysis,⁹ a reverse micelles route,¹⁰ combustion synthesis,¹¹ and sonochemical and microwave-assisted heating routes^{12,13} to name just a few.

Despite the high interest in the development of new methods to prepare nanocrystalline CeO₂, up to now, however, the surface properties and consistently the surface

* Corresponding author: tel ++39-049-8275196; fax ++39-049-8275161; e-mail martamaria.natile@unipd.it.

(1) Trovarelli, A. *Catal. Rev. Sci. Eng.* **1996**, *38*, 439 and references therein.
 (2) Minh, N. Q.; Takahashi, T. In *Science and Technology of Ceramic Fuel Cells*; Elsevier: New York, 1995.

(3) Klabunde, K. In *Nanoscale Materials in Chemistry*; Wiley-Interscience: New York, 2001 and references therein.
 (4) Hirano, M.; Kato, E. *J. Am. Ceram. Soc.* **1996**, *79*, 777.
 (5) Hirano, M.; Fukuda, Y.; Iwata, H.; Hotta, Y.; Inagaki, M. *J. Am. Ceram. Soc.* **2000**, *83*, 1287.
 (6) Zhou, Y.; Rahaman, M. N. *Acta Mater.* **1997**, *45*, 3635.
 (7) Chu, X.; Chung, W.; Schmidt, L. D. *J. Am. Ceram. Soc.* **1993**, *76*, 2115.
 (8) Chen, P. L.; Chen, I. W. *J. Am. Ceram. Soc.* **1993**, *76*, 1577.
 (9) Mädler, L.; Stark, W. J.; Pratsinis, S. E. *J. Mater. Res.* **2002**, *17*, 1356.
 (10) Masui, T.; Fujiwara, K.; Machida, K.; Adachi, G.; Sakata, T.; Mori, H. *Chem. Mater.* **1997**, *9*, 2197.
 (11) Mokkelbost, T.; Kaus, I.; Grande, T.; Einarsrud, M.-A. *Chem. Mater.* **2004**, *16*, 5489.
 (12) Wang, H.; Zhu, J. J.; Zhu, J. M.; Liao, X. H.; Xu, S.; Ding, T.; Chen, H. Y. *Phys. Chem. Chem. Phys.* **2002**, *4*, 3794.
 (13) Liao, X. H.; Zhu, J. M.; Zhu, J. J.; Xu, J. Z.; Chen, H. Y. *Chem. Commun.* **2001**, 937.

reactivity of the nanostructured CeO₂ obtained by means of different procedures (with particular reference to the evaluation of the distribution of active sites, the interaction mechanism, and the reaction paths) have not been sufficiently investigated.

This paper is part of a comprehensive work aiming to understand the reactivity of several ceria-based nanocomposite oxide systems, which are very promising in materials technology. Herein two synthetic procedures are used to prepare CeO₂ powders. CeO₂ is obtained by precipitation from a basic solution and by a microwave-assisted heating hydrolysis method. Compared with the first method, microwave synthesis has the advantage of very short reaction times, production of small particles with a narrow particle size distribution, and high purity.¹³ Jansen et al.¹⁴ suggested that these advantages could be attributed to fast homogeneous nucleation and ready dissolution of the gel.

The influence of the preparation procedure on the bulk and surface properties is deeply investigated. In particular, the effects of the synthesis and thermal treatment on structure, morphology, particle sizes, specific surface area, surface hydroxylation, and surface chemical composition are observed and discussed in connection to the powder reactivity. A particular attention is turned to the characterization of the surface active sites and to the study of the surface reactivity. In this regard the interaction of the powder samples with methanol is studied. Methanol, in fact, is an important probe molecule as well as an interesting combustible for fuel cell. To better understand the interaction of different samples with methanol, the active sites distributed on the sample surfaces are investigated by means of probe molecules (pyridine and carbon dioxide, respectively, for acidic and basic sites).^{15–20} It is important to underline that the authors have decided to study the active sites and the reactivity of the samples as prepared, avoiding any activation or cleaning treatment.

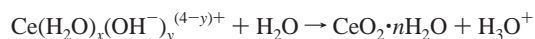
Experimental Section

(a) Synthesis: (i) Preparation of the CeO₂ Powder by Precipitation from a Basic Solution. CeO₂ was prepared by precipitation from a basic solution of cerium nitrate hexahydrate, Ce(NO₃)₃·6H₂O (Strem Chemicals, 99.9%). The solution was obtained dissolving the nitrate in distilled water and adding, under vigorous stirring, NH₃ (AnalaR 25%) until pH = 10.^{6,21} The precipitated Ce(OH)₃ was filtered out and washed with distilled water until NH₄⁺ and NO₃⁻ ions were entirely eliminated; then it was dried at 373 K for 5 h and calcined at two different temperature, 523 and 923 K, for 5 h in air.

(ii) Preparation of the CeO₂ Powder by Microwave-Assisted Heating Hydrolysis. CeO₂ was prepared by microwave-assisted

heating of an aqueous solution of 0.01 mol L⁻¹ [(NH₄)₂Ce(NO₃)₆], containing 1 wt % poly(ethylene glycol) 2000 (PEG) and 1 wt % sodium acetate (NaOOCCH₃).¹³ The prepared aqueous solution (pH = 4.4) was put in a quartz vessel into the microwave reaction system under pressure less than 100 bar. The microwave system (Milestone Ethos 1600) operates at 2450 MHz frequency. Several tests were done by varying systematically the microwave parameters such as temperature and hold time in order to find the lowest temperature and shortest time for the formation of the material. Then the solution was treated under microwaves for 10 min at 363 K (350 W).

The proposed mechanism of microwave-assisted heating hydrolysis preparation of the CeO₂ nanoparticles may be similar to a general hydrolysis process:¹³ first, hydrated Ce(IV) ions can form complexes with H₂O molecules or OH⁻ ions. Polymers of this hydroxide, Ce(H₂O)_x(OH⁻)_y^{(4-y)+}, can then serve as a precursor of the oxide. The starting precipitate from the Ce(IV) salt may be formed by nucleation of hydrated Ce(H₂O)_x(OH⁻)_y^{(4-y)+}, so leading to very fine precursors for the final oxide. In aqueous solution, water, as a polar molecule tends to take protons away from coordinated hydroxide and the reaction equation can be expressed by⁴



In the microwave heating environment, the fast, homogeneous heating gives rise to a rapid and more simultaneous nucleation than the conventional method. Consequently uniformly small particles can be prepared. PEG, as a dispersion stabilizer, can inhibit nonhomogeneous precipitation to obtain homogeneous precipitation. Sodium acetate is used to adjust the pH of the solution. The resulting precipitate, cooled to room temperature, was centrifuged, washed with distilled water several times and finally dried at 373 K for 5 h. The final yellow product was calcined at 523 K for 5 h in air.

(b) XPS Measurements. X-ray photoelectron spectra (XPS) were recorded on a Perkin-Elmer PHI 5600ci spectrometer with a standard Al K α source (1486.6 eV) working at 350 W. The working pressure was less than 1 \times 10⁻⁸ Pa. The spectrometer was calibrated by assuming the binding energy (BE) of the Au 4f_{7/2} line to lie at 84.0 eV with respect to the Fermi level. Extended spectra (survey) were collected in the range 0–1350 eV (187.85 eV pass energy, 0.4 eV step, 0.05 s step⁻¹). Detailed spectra were recorded for the following regions: C 1s, O 1s, Ce 3d, and Ce 4d (11.75 eV pass energy, 0.1 eV step, 0.1 s step⁻¹). The standard deviation in the BE values of the XPS line is 0.10 eV. The atomic percentage, after a Shirley type background subtraction,²² was evaluated by use of the PHI sensitivity factors.²³ To take into consideration charging problems, the C 1s peak at 285.0 eV was considered and the peaks' BE differences were evaluated.

The sample for the XPS analysis was processed as a pellet by pressing the catalyst powder at ca. 7 \times 10⁶ Pa for 10 min; the pellet was then evacuated for 12 h at ca. 1 \times 10³ Pa.

(c) Diffuse Reflectance Infrared Fourier Transform (DRIFT) Measurements and Reaction Conditions. The IR spectra were collected in a Bruker IFS 66 spectrometer (accumulating 128 scans at a resolution of 4 cm⁻¹) and displayed in Kubelka–Munk units.^{24,25} The temperature of the powder was checked by means of a thermocouple inserted into the sample holder directly in contact with the powder.

(14) Jansen, J. C.; Arafat, A.; Barakat, A. K.; Van Bekkum, H. In *Synthesis of Microporous Materials*; Ocelli, M. L., Robson, H., Eds.; Van Nostrand Reinhold: New York, 1992.

(15) Parry, E. P. *J. Catal.* **1963**, *2*, 371.

(16) Little, L. H. In *Infrared Spectra of Adsorbed Species*; Academic Press: San Diego, CA, 1966; Chapt. 7.

(17) Nortier, P.; Furre, P.; Mohammed Saad, A. B.; Saur, O.; Lavalley, J. C. *Appl. Catal.* **1990**, *61*, 141.

(18) Busca, G. *Catal. Today* **1998**, *41*, 191.

(19) Auroux, A.; Gervasini, A. *J. Phys. Chem.* **1990**, *94*, 6371.

(20) Rethwisch, D. G.; Dumesic, J. A. *Langmuir* **1986**, *1–2*, 73.

(21) Li, C.; Domen, K.; Maruya, K.; Onishi, T. *J. Am. Chem. Soc.* **1989**, *111*, 7683.

(22) Shirley, D. A. *Phys. Rev.* **1972**, *55*, 4709.

(23) Moulder, J. F.; Stickle, W. F.; Sobol, P. E.; Bomben, K. D. In *Handbook of X-ray Photoelectron Spectroscopy*; Chastain, J., Ed.; Physical Electronics: Eden Prairie, MN, 1992.

(24) Kubelka, P.; Munk, F. *Z. Tech. Phys.* **1931**, *12*, 593.

(25) Kortum, G. *Reflectance Spectroscopy*; Springer: New York, 1969.

Prior to each experiment, ca. 50 mg of the sample was loaded in the sample cup of a low-temperature reaction chamber (CHC) installed in the Praying Mantis accessory for diffuse reflection spectroscopy (Harrick Scientific Corp.) and fitted with ZnSe windows; the powder was kept in nitrogen flow to eliminate water traces until a stable IR spectrum was obtained (ca. 2 h). Then, the sample was exposed to the reactive species at a flow rate of 100–150 cm³ min⁻¹, before measurement. The background spectrum of the clean surface was measured for spectra correction.

The CHC chamber was filled with the pyridine or the alcohol vapors flowing nitrogen through a bubbler containing the liquid, whereas for CO₂ (Air Liquide, 99.998%) the gas outlet was directly connected to the reaction chamber. Pyridine and methanol used for the chemisorption were taken from a commercial source (Sigma–Aldrich, spectroscopic grade) and used without further purification.

(d) Thermal Analysis and XRD. Thermogravimetric analysis (TGA) was carried out in a controlled atmosphere by use of the simultaneous differential techniques (SDT) 2960 of TA Instruments. Thermograms were recorded at 5 K min⁻¹ heating rate in air and in nitrogen flow. The temperature ranged from room temperature (RT) to 1273 K.

X-ray diffraction (XRD) patterns were obtained with a Bruker D8 Advance diffractometer with Bragg–Brentano geometry and Cu K α radiation (40 kV, 40 mA, $\lambda = 0.154$ nm).

(e) TEM and EDS. Transmission electron micrographs were obtained with a Philips JRM 2010 electron microscope using 200 kV primary voltage. The samples used for TEM observations were prepared by dispersing some products in ethanol followed by ultrasonic vibration for 30 min and then placing a drop of the dispersion onto a copper grid (200 Cu) coated with a layer of amorphous carbon. Energy-dispersive spectroscopy (EDS) measurements were carried out by means of a LINK INCA 100 microanalysis system. The diameter of the analyzed spot was 5–15 nm.

(f) Specific Surface Areas. N₂ adsorption isotherms at 77 K were measured on a Micrometrics ASAP 2010 system. The sample was previously evacuated at different temperatures down to a pressure of 2 Pa. The specific surface area was determined by evaluating the equilibrium points inside the 0.05–0.33 p/p_0 range by the Brunauer–Emmett–Teller (BET) equation.²⁶ The pore size distribution was calculated by the Barret–Joyner–Halenda (BJH) method,²⁷ with the Harkins and Jura equation²⁸ for multilayer thickness.

Results and Discussion

(a) CeO₂ Characterization. All the CeO₂ powders were characterized by X-ray diffraction (XRD) (Figure 1). The XRD patterns show the reflections characteristic of CeO₂ cubic phase with fluorite structure. Concerning the two samples obtained by precipitation, it is noteworthy that the sample heated at higher temperature is characterized by narrower peaks than the one treated at 523 K. This suggests an increase of particle diameter with increasing heating temperature. The average diameter of the two CeO₂ samples prepared by precipitation, evaluated by means of the Scherrer formula,²⁹ is about 9 nm for the CeO₂ calcined at 523 K and 12 nm for the one calcined at 923 K. The more evident

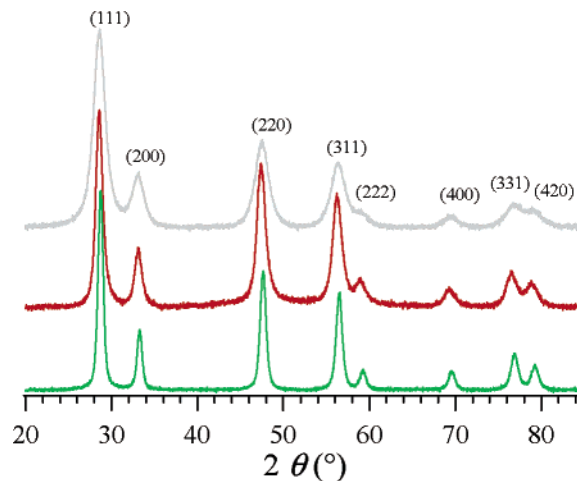


Figure 1. XRD patterns of the two CeO₂ samples prepared by precipitation and treated at 523 K (red) and 923 K (green) and of the CeO₂ prepared by microwave irradiation and treated at 523 K (gray).

broadness of the peaks observed on the sample obtained by microwave-assisted heating suggests a smaller crystallite size as well as a lower crystallinity: the particle diameter is around 6 nm.

The increase of particle sizes with increasing temperature of the thermal treatment in the two CeO₂ samples obtained by precipitation is evident also in TEM images (Figure 2). TEM images, in fact, reveal a broad particle distribution; the diameter of the ceria particles is around 8.0–10.0 nm for the sample heated at 523 K and around 12.0–15.0 nm for the one heated at 923 K. These results are in agreement with the values obtained by means of the Scherrer formula.

Smaller particles with a narrow particle size distribution (average diameter around 3.3–4.0 nm) characterize the CeO₂ obtained in microwave (Figure 3). The CeO₂ prepared by microwave-assisted heating shows a higher specific surface area than the analogous one obtained by precipitation (Table 1). The two samples show also different porosities: the sample obtained in microwave is constituted mainly of micropores (average diameter less than 2.0 nm), with only a few mesopores having an average diameter of about 7.1 nm observed; the one obtained by precipitation is characterized by mesopores, ranging around 9.1 nm. Consistently pores of smaller volume characterize the former. Concerning the two samples prepared by precipitation, the heat treatment at 923 K causes the specific surface area to decrease from 58 to 41 m²/g. Consistently also the pore volume decreases. The pore size of the sample treated at 923 K ranges around 11.2 nm.

The XP extended spectra (survey) do not reveal the presence of species different from the expected ones (i.e., Ce, O, C). This is also confirmed by EDS analysis. The XP detailed spectra obtained for the powder oxides are shown in Figure 4, whereas the peak positions are summarized in Table 2. It is worth underlining that minimum time of exposure (determined by means of repeated measures at increasing irradiation time) was used to avoid ceria reduction under XPS conditions, which is well documented in literature.³¹

The Ce 3d level has a very complicated structure: six peaks corresponding to three pairs of spin–orbit doublets

(26) Gregg, S. J.; Sing, K. S. W. *Adsorption, Surface Area and Porosity*; Academic Press: London, 1982.

(27) Barret, E. P.; Joyner, L. G.; Halenda, P. P. *J. Am. Chem. Soc.* **1951**, *73*, 373.

(28) Harkins, W. D.; Jura, G. *J. Am. Chem. Soc.* **1944**, *66*, 1366.

(29) Enzo, S.; Polizzi, S.; Benedetti, A. *Z. Kristallogr.* **1985**, *170*, 275.

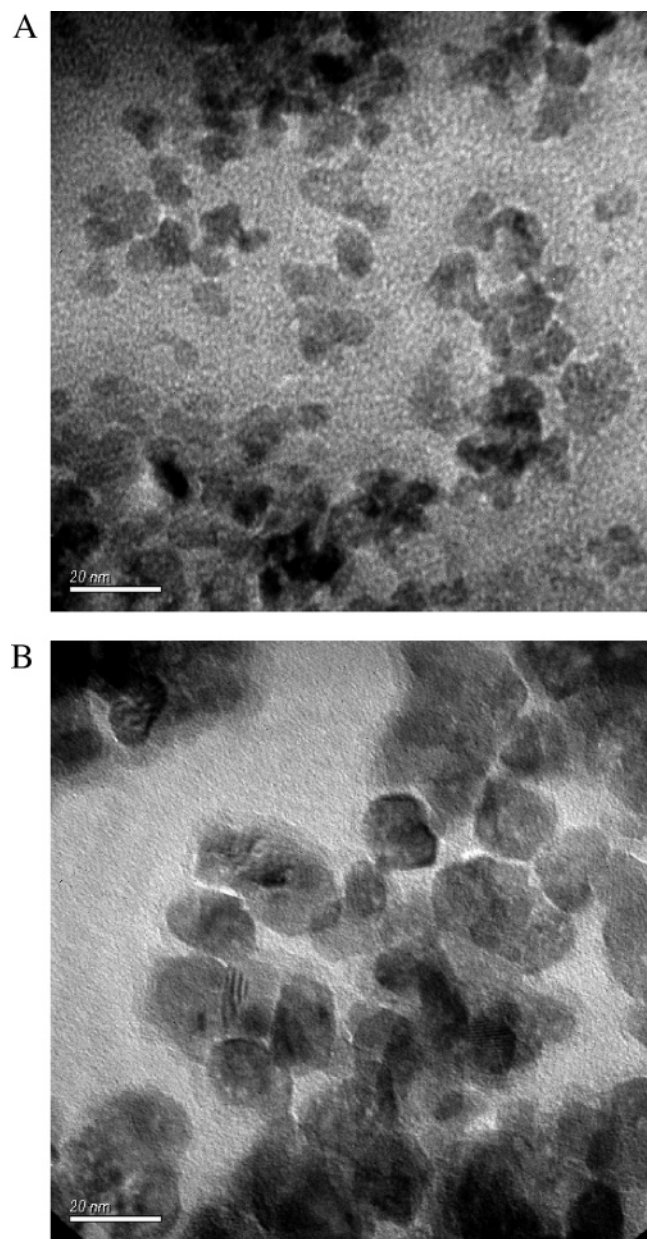


Figure 2. TEM images of the CeO₂ obtained by precipitation and heated at (A) 523 K and (B) 923 K.

[noted as (V, U), (V'', U''), and (V''', U''')] can be identified in the Ce 3d spectrum of Ce(IV) oxide,^{33,34} while four peaks due to two pairs of doublets [noted as (V^o, U^o) and (V', U')] characterize the Ce 3d spectrum of Ce(III) oxide.³³ The labels follow the convention established by Burroughs et al.:³⁵ V⁽ⁿ⁾ and U⁽ⁿ⁾ refer to the 3d_{5/2} and 3d_{3/2} spin-orbit component, respectively. The Ce 3d peak positions (signals V, V'', U, U'' and U'''; Figure 4) agree with literature data for CeO₂ (Table 2). XP analysis reveals a slight reduction

- (30) Praline, G.; Koel, B. E.; Hance, R. L.; Lee, H. I.; White, J. M. *J. Electron Spectrosc. Relat. Phenom.* **1980**, *21*, 17.
 (31) Park, P. W.; Ledford, J. S. *Langmuir* **1996**, *12*, 1794.
 (32) Rama Rao, M. V.; Shripathi, T. *J. Electron Spectrosc. Relat. Phenom.* **1997**, *87*, 121.
 (33) Mullins, D. R.; Overbury, S. H.; Huntley, D. R. *Surf. Sci.* **1998**, *409*, 307.
 (34) Paparazzo, E.; Ingo, G. M.; Zacchetti, N. *J. Vac. Sci. Technol., A* **1991**, *9*, 1416.
 (35) Burroughs, P.; Hammet, A.; Orchard, A. F.; Thornton, G. *J. Chem. Soc., Dalton Trans.* **1976**, 1686.

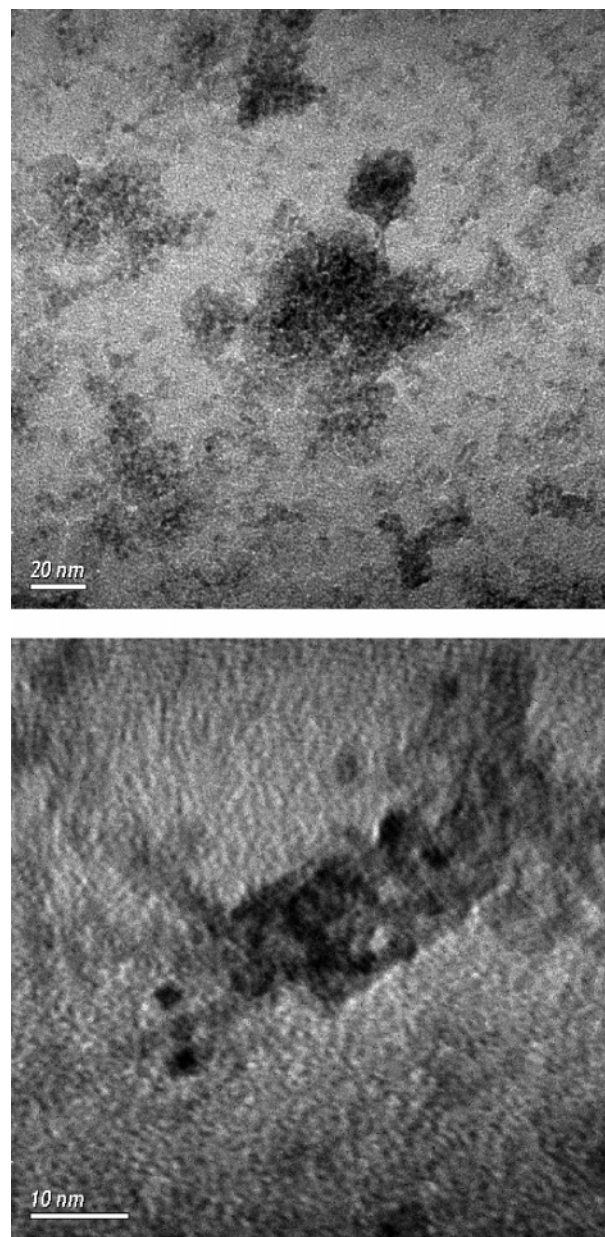


Figure 3. TEM images of the CeO₂ obtained by microwave irradiation and treated at 523 K.

Table 1. Specific Surface Area, Pore Volume, and Pore Diameter of CeO₂^a

sample	specific surface area (m ² /g)	pore volume (cm ³ /g)	pore diameter (nm)
CeO ₂ mw (523 K)	72 ± 1	0.0104	<2.0; 7.1
CeO ₂ (523 K)	58 ± 1	0.1196	9.1
CeO ₂ (923 K)	41 ± 1	0.1142	11.2

^a Measured for the CeO₂ prepared by microwave-assisted heating and treated at 523 K and for the two CeO₂ samples prepared by precipitation and treated at 523 and 923 K, respectively.

of the surface of the CeO₂ obtained by microwave-assisted heating with respect to the ceria obtained by precipitation and treated at the same temperature. Beyond the peaks characteristic of Ce(IV), in fact, the contributions V' and U', characteristic of Ce(III), are well evident.^{31,32} The detailed investigation of the Ce 4d spectral region confirms the sample reduction: the X''' and W''' contributions characteristic of Ce(IV) are more intense in the CeO₂ obtained by precipitation and treated at 523 K (Figure 4).³³ Moreover, because the

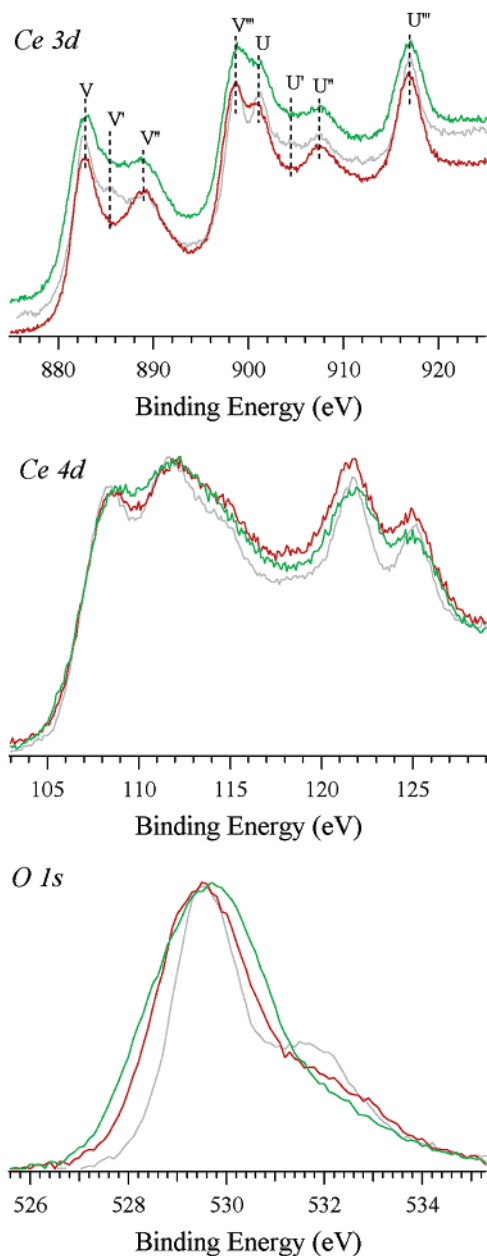


Figure 4. Ce 3d, Ce 4d and O 1s XP spectra of the two CeO₂ samples prepared by precipitation and treated at 523 K (red) and 923 K (green) and of the CeO₂ prepared by microwave irradiation (gray). The spectra are normalized with respect to their maximum values.

escape depth is higher for Ce 4d than Ce 3d photoelectrons,³⁶ it is evident that the reduction phenomenon does not interest only the outer layers. This higher reduction degree of the surface of the CeO₂ obtained by microwave-assisted heating can be due to the lower particle dimensions. Several studies, in fact, show that the energy required to reduce ceria increases with particle sizes.³⁷ Moreover, the reduction of the ceria nanoparticles is structure-sensitive, being easier in systems that have a low degree of crystallinity.³⁸

Among the three samples, the one obtained by precipitation and heated at 923 K is characterized by the most reduced surface: the contributions distinctive of Ce(III) are much

Table 2. XPS Peak Positions Obtained for the CeO₂ Samples^a

XPS peak	CeO ₂ (523 K)	CeO ₂ (923 K)	CeO ₂ mw (523 K)	CeO ₂ ^b	Ce ₂ O ₃ ^b	
Ce 3d _{5/2}	V	882.9	883.2	882.7	882.6	
	V		885.6	885.5		885.4
	V	889.0	888.7	889.1	888.6–889.3	
	V	898.7	899.1	898.7	898.3–898.5	
Ce 3d _{3/2}	U	900.8	901.0	901.1	900.4–900.8	
	U		904.5	904.5		903.9–904.1
	U	907.4	907.4	907.4	906.3–907.8	
	U	916.8	916.9	916.9	916.6–916.8	
Ce 4d	A	108.9	108.8	108.5	109.3	
	B	112.1	111.9	111.7	112.6	
	C				115.7	
	X	121.7	121.7	121.7	122.8	
	W	124.9	124.7	125.0	126.1	
	O 1s	Ce–O	529.6	529.7	529.5	529.0–530.4
	Ce–OH	531.6	531.6	531.6	531.6	

^a XPS peak positions (binding energies) are given in electronvolts.

^b Literature values are also reported, from refs 30–33.

more pronounced (Figure 4, see Ce 3d and Ce 4d regions). In this case the temperature of heat treatment seems to be responsible for the sample reduction. The temperature effect has been investigated by comparing the Ce 3d and Ce 4d spectra obtained on several CeO₂ samples prepared by precipitation from a basic solution and calcined at different temperatures (523, 723, 923, and 1123 K): the contributions characteristic of Ce(III) become more and more evident with temperature increase.

The position of the O 1s XP peak (Figure 4) in all the three samples (529.6–529.7 eV) agrees with the expected value for oxygen in ceria (Table 2). The fitting procedure also shows a contribution at higher BE (around 531.6 eV) attributed to the presence of hydroxyl groups.³⁹ The shape of the O 1s peaks, however, suggests a different distribution of hydroxyl groups in the three samples.

The slight narrowing of the signals of the CeO₂ obtained by microwave-assisted heating in the “U region” could suggest a chemical and/or structural reordering phenomenon. The same behavior was observed in the Ce 4d and O 1s XP spectral regions (Figure 4). This result agrees with the narrow particle size distribution observed in TEM images.

The O/Ce atomic ratio calculated with respect to Ce 3d XP peak is 1.8 and 1.7 for the two samples prepared by precipitation and heated at 523 and 923 K, respectively, while it is 1.95 for the CeO₂ obtained by microwave irradiation. These results confirm that the CeO₂ prepared by precipitation and heated at 923 K is characterized by a higher reduction degree than the one obtained by microwave.

The DRIFT spectra recorded from RT to 673 K for the three CeO₂ samples are reported in Figures 5–7. At RT the intense and broad band observed in the O–H stretching region of all three samples is mainly due to H-bound hydroxyl groups and to molecularly chemisorbed water (Figures 5a, 6a and 7a). The last presence is confirmed by the corresponding bending around 1628 cm⁻¹ (Figures 5b, 6b, and 7b). Three different contributions are also evident on the CeO₂ treated at 923 K: the peak at 3692 cm⁻¹ is probably due to different adsorbed water molecules,^{40–42} and in fact it rapidly disappears when temperature increases;

(36) Seah, M. P.; Dench, W. A. *Surf. Interface Anal.* **1979**, *1*, 2.

(37) Cordatos, H.; Ford, D.; Gorte, R. J. *J. Phys. Chem.* **1996**, *100*, 18128.

(38) Fernandez-Garcia, M.; Martinez-Arias, A.; Hanson, J. C.; Rodriguez, J. A. *Chem. Rev.* **2004**, *104*, 4063.

(39) McIntyre, N. S.; Chan, T. C. In *Practical Surface Analysis 1*, 2nd ed.; Briggs, D., Seah, M. P., Eds.; Wiley: Chichester, U.K., 1990; Chapt. 10.

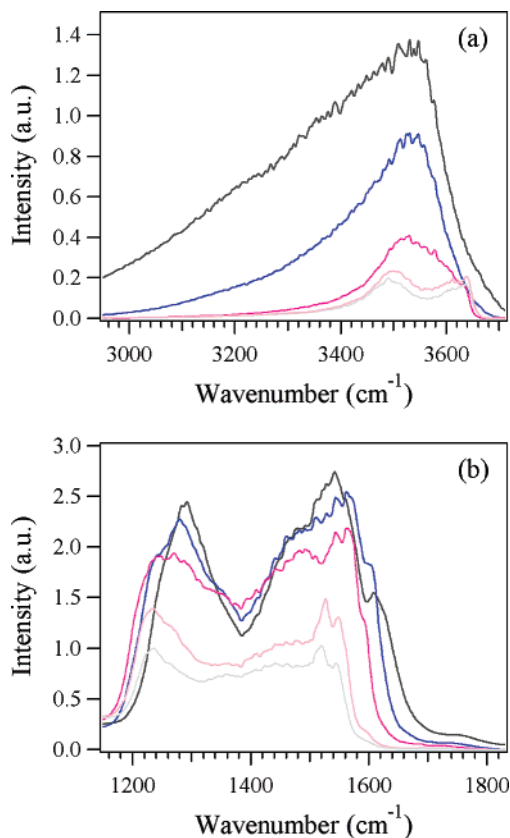


Figure 5. DRIFT spectra of the CeO₂ prepared by precipitation and heated at 523 K recorded at different temperatures: (black) RT, (blue) 373 K, (magenta) 523 K, (pale pink) 623 K, and (gray) 673 K. (a) spectral region from 2950 to 3710 cm⁻¹; (b) spectral region from 1150 to 1830 cm⁻¹.

while the contributions at 3633 and 3663 cm⁻¹ are characteristic of two different bicoordinated hydroxyl groups. In particular, the difference between these two bicoordinated hydroxyl species is due to their coordination to cerium cations with a different unsaturation degree.⁴⁰

The heat treatment causes the desorption of molecularly chemisorbed water molecules as well as the condensation of H-bound hydroxyl groups, while signals characteristic of isolated hydroxyl groups become more and more evident. The broad tail of the hydroxyl stretching band at low wavenumber progressively disappears: this phenomenon is more evident in the two CeO₂ samples prepared by precipitation, suggesting the presence of stronger bound water molecules (as water chemisorbed on the Lewis acidic sites) on the sample prepared by microwave. At 573 K on the CeO₂ obtained by precipitation and heated at 523 K, two peaks characteristic of tri- (3514 cm⁻¹) and bicoordinated (3636 cm⁻¹)^{40,43} hydroxyl groups start to be revealed. The same contributions were observed from 373 K in the sample prepared by microwave. At higher temperature these two contributions become more and more clear. Upon increasing

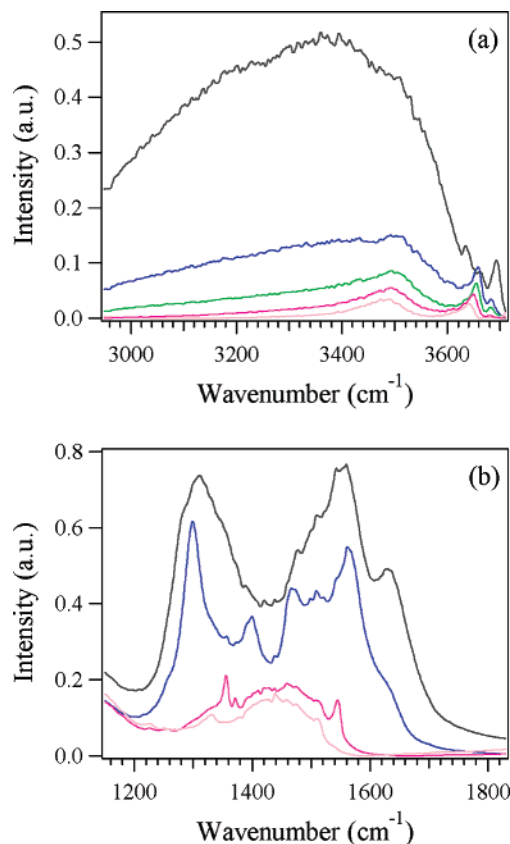


Figure 6. DRIFT spectra of the CeO₂ prepared by precipitation and heated at 923 K recorded at different temperatures: (black) RT, (blue) 373 K, (green) 423 K, (magenta) 523 K, and (pale pink) 623 K. (a) Spectral region from 2950 to 3710 cm⁻¹; (b) spectral region from 1150 to 1830 cm⁻¹.

the temperature, both the peaks at 3514 and 3636 cm⁻¹ decrease in intensity and shift toward lower wavenumber, suggesting a decrease of lateral interaction.⁴⁴

Concerning the CeO₂ treated at 923 K, the heating at 373 K leads to a striking variation in the higher wavenumber spectral range: the contributions at 3633 and 3663 cm⁻¹ disappear, and two peaks at 3658 and 3682 cm⁻¹ become evident. The former could be due to bicoordinated species, which owing to the desorption of molecular chemisorbed water as well as the condensation of the H-bound hydroxyl groups become more evident. With regard to the signal at 3682 cm⁻¹ Badri et al.⁴⁰ observed similar values for hydroxyl groups bicoordinated to reduced ceria. The presence of hydroxyl groups coordinated to Ce(III) cations agrees with XPS outcomes indicating that the CeO₂ obtained by precipitation and heated at 923 K is characterized by a higher reduction degree than the one prepared by microwave-assisted heating. At 373 K also the peak of tricoordinated hydroxyl groups (around 3500 cm⁻¹) begins to be visible on the CeO₂ treated at 923 K. Upon heating at higher temperature, all the peaks show a progressive decrease of intensity. At the same time the shift of the peak of the bicoordinated hydroxyl groups from 3658 to 3640 cm⁻¹ suggests that the dehydration of the surface favors the creation of oxygen vacancies and consequently of hydroxyl groups bicoordinated to coordinatively unsaturated cerium cations.⁴⁰

(40) Badri, A.; Binet C.; Lavalley, J. C. *J. Chem. Soc., Faraday Trans.* **1996**, *92*, 4669.

(41) Binet, C.; Daturi, M.; Lavalley, J.-C. *Catal. Today* **1999**, *50*, 207.

(42) Daturi, M.; Finocchio, E.; Binet, C.; Lavalley, J.-C.; Fally, F.; Perrichon, V. *J. Phys. Chem. B* **1999**, *103*, 4884.

(43) Laachir, A.; Perrichon, V.; Badri, A.; Lamotte, J.; Batherine, E.; Lavalley, J. C.; El Fallah, J.; Hilaire, L.; LeNormand, F.; Quéméré, E.; Sauvion, G. N.; Touret, O. *J. Chem. Soc., Faraday Trans.* **1991**, *87*, 1601.

(44) Zecchina, A.; Lamberti, C.; Bordiga, S. *Catal. Today* **1998**, *41*, 169.

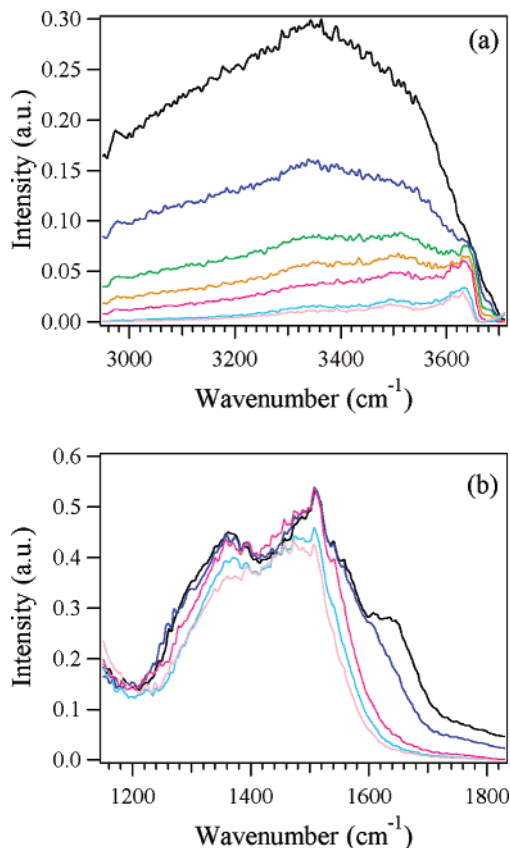


Figure 7. DRIFT spectra of the CeO₂ prepared by microwave irradiation and heated at 523 K recorded at different temperatures: (black) RT, (blue) 373 K, (green) 423 K, (orange) 473 K, (magenta) 523 K, (pale blue) 573 K, and (pale pink) 623 K. (a) Spectral region from 2950 to 3710 cm⁻¹; (b) spectral region from 1150 to 1830 cm⁻¹.

A broad envelope of bands below 1830 cm⁻¹ (Figures 5b, 6b, and 7b) in all three samples indicates the presence (beyond the hydroxyl bending peak) of several contributions ascribed to different carbonate species. The presence of these species is rather usual in ceria and ceria-based materials and has to be related to the interaction with atmospheric carbon dioxide.⁴⁵ In the O–C–O spectral range of the sample prepared by precipitation and treated at 523 K, several signals can be observed. The comparison with literature data suggests the presence of monodentate (1490 cm⁻¹)⁴⁶ and three different bidentate (1283 and 1561, 1292 and 1543, 1242 and 1528 cm⁻¹) carbonate species.⁴⁷ On the sample heated at 923 K, beyond mono- (1399, 1477 cm⁻¹) and bidentate (1310 and 1560, 1356 and 1543 cm⁻¹) carbonate species, the presence of inorganic carboxylate (1509 cm⁻¹)^{41,46–48} was observed. Also, on the CeO₂ prepared by microwave, the positions and spectral shape suggest the presence of several carbonate species.

With regard to the samples obtained by precipitation (Figures 5b and 6b), the heat treatment causes a severe decrease of the signals attributed to carbonate species, suggesting a weak interaction between carbon dioxide and

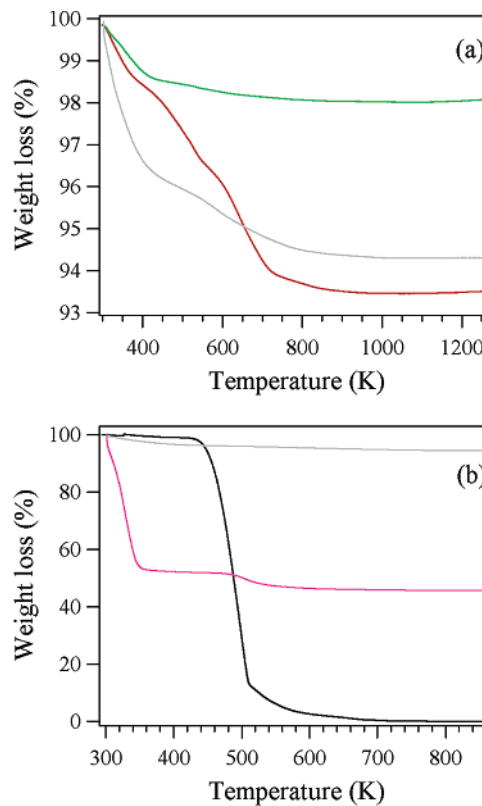


Figure 8. (a) TG spectra (recorded in N₂) of the two samples prepared by precipitation and treated at 523 K (red) and 923 K (green) and of the one prepared by microwave irradiation and treated at 523 K (gray). (b) TG spectra (recorded in N₂) of PEG-2000 (black) and of the CeO₂ obtained by microwave irradiation before (magenta) and after (gray) the heat treatment at 523 K.

surface active sites. This behavior is particularly evident in the sample treated at higher temperature. On the contrary, the heat treatment does not significantly modify the O–C–O spectral range of the CeO₂ prepared by microwave, suggesting a strong interaction between carbon dioxide and surface active sites.

Thermal analysis was carried out in both nitrogen and air flow without significant differences. The TG spectra of the three samples are compared in Figure 8a. The investigation of the TG spectra of the two samples treated at 523 K reveals several differences. The CeO₂ prepared by microwave-assisted heating shows a significant water loss at $T < 400$ K and a quite low and continuous weight loss due to the condensation of hydroxyl groups until about 850 K. The sample prepared by precipitation, instead, shows a significant weight decrease due to water desorption and condensation of hydroxyl groups between RT and about 850 K. Concerning this last sample, the weight loss due to the decomposition of carbonate species cannot be excluded, as suggested also by the DRIFT outcomes. The thermal analysis results are very different for the two samples treated at 523 K and the one heated at 923 K (Figure 8a). The latest sample, in fact, reveals a quite weak and continuous weight loss.

Figure 8b shows the TG spectra (recorded in N₂) of PEG-2000 and of the CeO₂ prepared by microwave-assisted heating before and after the thermal treatment at 523 K. Investigation of the TG spectra reveals that PEG decomposes at 484 K, but when CeO₂ is present the decomposition takes place at about 504 K. Moreover, in this last case a significant

(45) Rosynek, M. P.; Magnuson, D. T. *J. Catal.* **1977**, *48*, 417.

(46) Li, C.; Sakata, Y.; Arai, T.; Domen, K.; Maruya, K.-I.; Onishi, T. *J. Chem. Soc., Faraday Trans. 1* **1989**, *85*, 4, 929.

(47) Li, C.; Sakata, Y.; Arai, T.; Domen, K.; Maruya, K.-I.; Onishi, T. *J. Chem. Soc., Faraday Trans. 1* **1989**, *85*, 6, 1451.

(48) Gatehouse, B. M.; Livingstone, S. E.; Nyholm, R. S. *J. Chem. Soc.* **1958**, 3137.

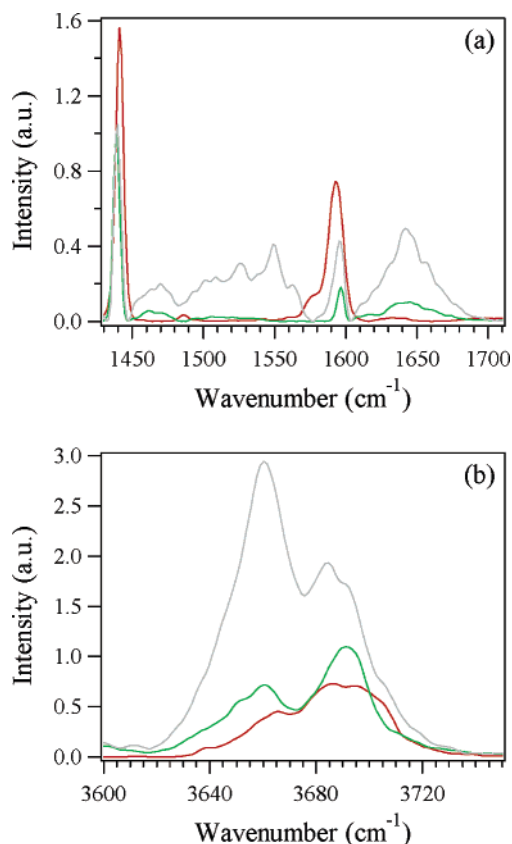


Figure 9. DRIFT spectra obtained at RT after exposure of the two samples prepared by precipitation and treated at 523 K (red) and 923 K (green) and the one prepared by microwave-assisted heating and treated at 523 K (gray) to pyridine + N₂ mixture. (a) Spectral region from 1430 to 1710 cm⁻¹; (b) spectral region from 3600 to 3750 cm⁻¹.

water loss is also observed before 350 K. The thermal spectrum of the CeO₂ before the heat treatment allows us to quantify the PEG in the sample at about 6.2%. After the thermal treatment, no traces of polymer are observed anymore. This demonstrates the absence of the polymer in the final product.

(b) Interaction with Pyridine and with CO₂. In Figure 9 the DRIFT spectra obtained after exposure of the three CeO₂ samples to pyridine + N₂ mixture at RT are shown. Concerning the CeO₂ sample obtained by precipitation and treated at 523 K (Figure 9a), the spectral region of the ring stretching modes reveals the presence of liquidlike pyridine and pyridine H-bound to the surface hydroxyl groups. This evidence is pointed out by the position and shape of the vibrational modes at 1441, 1486, 1576, and 1593 cm⁻¹ (Figure 9a).^{15,49,50}

Acidic sites were observed on the CeO₂ obtained by precipitation and calcined at 923 K and even more on the sample prepared by microwave-assisted heating. The broad and intense band above 1600 cm⁻¹ confirms their presence (Figure 9a). This complex band envelope is made up of several contributions at 1610, 1617, and 1637 cm⁻¹ and at wavenumbers higher than 1644 cm⁻¹. The contributions at 1610, 1617, and 1637 cm⁻¹ can be ascribed to pyridine interacting with Lewis acidic sites characterized by different

strengths.^{51,52} These can be constituted by coordinatively unsaturated cerium cations or cerium cations in a different oxidation state [Ce(IV) and Ce(III)]. At higher wavenumber (higher than 1644 cm⁻¹) is expected to fall the 8a vibrational mode of pyridine interacting with Brønsted acidic sites.^{15,50} The contribution around 1550 cm⁻¹ in the spectrum of the CeO₂ obtained by microwave-assisted heating confirms this presence. The formation of protonated species in the CeO₂ obtained by microwave irradiation indicates the presence of strong Brønsted acidic surface sites. The broadening of the band above 1600 cm⁻¹ toward higher wavenumber could suggest also the formation of the oxidation species (α -pyridone, as an example, was observed to range from 1650 to 1680 cm⁻¹ by Zaki et al.⁵¹).

The contributions due to pyridine interacting by H-bond with the surface hydroxyl groups are also observed (peaks at 1439 and 1597 cm⁻¹)^{51,52} on the two reduced CeO₂ samples.

After evacuation at RT, the bands due to liquidlike and H-bound pyridine progressively decrease, while the contributions above 1600 cm⁻¹ remain almost unchanged, suggesting that the pyridine coordinated to Lewis and Brønsted acidic sites is very strongly tied up. This confirms the presence of medium- to high-strength acidic sites.

Parallel to the above spectral changes, pyridine interaction brings about a severe perturbation of the surface hydroxyl groups by creating a broad adsorption around 3620–3730 cm⁻¹ (Figure 9b). Both the pyridine interacting by H-bond and pyridine species coordinated to Lewis and Brønsted acidic sites may be responsible for the perturbation. As an example, one of the most common mechanisms of interaction of Lewis-coordinated pyridine with hydroxyl groups is through an H-bond between a pyridine π -cloud and hydroxyl groups.⁵³

The above-mentioned DRIFT results indicate that the H-bound pyridine is the only species accountable for the hydroxyl perturbation on the CeO₂ prepared by precipitation and treatment at 523 K; on the contrary, the pyridine interacting with Lewis and Brønsted acidic sites is mainly responsible for the perturbation on the other two samples. It is interesting to note that, with increasing amounts of Lewis and Brønsted acidic sites, the intensity of the perturbation increases: it is higher for the CeO₂ obtained by microwave-assisted heating than for the CeO₂ prepared by precipitation and treated at 923 K. Moreover, it seems that the pyridine perturbs different kind of hydroxyl groups. The broad band is made up of two contributions at 3660 and 3685 cm⁻¹ ascribable to hydroxyl groups bicoordinated to Ce(IV) and Ce(III) cations, respectively.⁴⁰ Pyridine interacting with the sample surface favors thus the release of free bicoordinated hydroxyl groups. It is interesting to observe that the hydroxyl groups bicoordinated to Ce(IV) cations are the main liberated species on the CeO₂ obtained by microwave-assisted heating, while the ones bicoordinated to Ce(III) cations prevail on

(49) Corrsin, L.; Fax, B. J.; Lord, R. C. *J. Phys. Chem.* **1953**, *21*, 1170.
 (50) Morterra, C.; Chiorino, A.; Ghiotti, G.; Fiscaro, E. *J. Chem. Soc., Faraday Trans. 1* **1982**, *78*, 2649.

(51) Zaki, M. I.; Hasan, M. A.; Al-Sagheer, F. A.; Pasupulety, L. *Colloids Surf., A* **2001**, *190*, 261.

(52) Zaki, M. I.; Hussein, G. A. M.; Mansour, S. A. A.; El-Ammawy, H. A. *J. Mol. Catal.* **1989**, *51*, 209.

(53) Morterra, C.; Ghiotti, G.; Bocuzzi, F.; Coluccia, S. *J. Catal.* **1978**, *51*, 299.

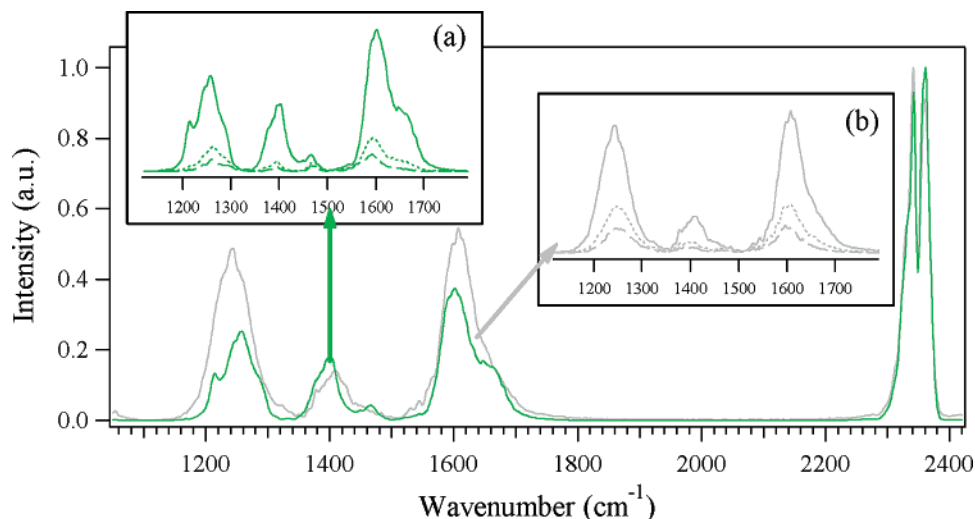


Figure 10. DRIFT spectra obtained at RT after exposure of the sample prepared by precipitation and treated at 923 K (green) and the one prepared by microwave-assisted heating and treated at 523 K (gray) to CO₂: spectral region from 1120 to 2420 cm⁻¹. In insets a and b, the spectra obtained after exposure to CO₂ and successively to N₂ for 3 min (dotted lines) and 15 min (dashed lines) are shown.

Table 3. FTIR Data of Vapor and Liquid Methanol and Methoxy Species Adsorbed on Unreduced and Reduced CeO₂^a

	CH ₃ OH _(g) ^c		unreduced CeO ₂ ^b			reduced CeO ₂ ^b		
	CH ₃ OH _(l) ^d		OCH ₃ (I)	OCH ₃ (II)	OCH ₃ (III)	OCH ₃ (I)	OCH ₃ (II)	OCH ₃ (III)
$\nu_a(\text{CH}_3)$	2973 vs	2934 vs	2911	2922	~2922		2920	
$2\delta(\text{CH}_3)$			2883					
$\nu_s(\text{CH}_3)$	2826	2822 s	2803	2793	2793		2780	
	2845 s		2808	2800	~2800			
	2869							
$\nu(\text{CO})$	1012	1029	1105	1065	1015	1117	1087	1040
	1034		1108	1054	1025		1077	1045
	1054			1042			1067	

^a FTIR data are given in reciprocal centimeters. I, II, and III indicate mono-, bi-, and tricoordinated methoxy species, respectively. ^b References 56–59. ^c References 54 and 55. ^d Reference 55.

the sample prepared by precipitation and treated at 923 K. This behavior agrees with the above-reported XPS and DRIFT outcomes.

DRIFT spectra recorded after the exposure of the CeO₂ sample obtained by precipitation and calcination at 523 K to CO₂ at RT does not indicate the presence of basic sites. CO₂ does not interact with the oxide surface to form carbonate species, because the active sites distributed on the surface have already reacted with the atmospheric carbon dioxide, giving rise to different carbonate species.

Figure 10 shows the DRIFT spectra collected after exposure of both the CeO₂ obtained by precipitation and calcination at 923 K and the one prepared by microwave-assisted heating to CO₂ at RT. The signals observed on the CeO₂ sample treated at 923 K agree with the formation of bi- (1215, 1257, 1593 cm⁻¹) and monodentate (1403 and 1467 cm⁻¹) carbonate species.^{46,47} A shoulder at wavenumber higher than 1593 cm⁻¹ suggests the presence of bicarbonate species.^{46,48} Similar results were obtained in the sample synthesized by microwave (1245, 1530, 1544, 1607, and 1410 cm⁻¹). This means the presence of basic active sites constituted by coordinatively unsaturated oxygen anions (giv-

ing rise to monodentate carbonate species) and of complex sites formed by a Lewis acidic site and its coordinatively unsaturated neighboring oxygen anion (originating a bidentate carbonate).

The intensity of the DRIFT spectra in the O–C–O spectral range after exposure to CO₂ is different. This suggests a higher amount of basic sites on the surface of the sample prepared by microwave.

N₂ removes almost completely all these species, suggesting a very weak interaction (Figure 10, insets a and b). This behavior is more evident in the CeO₂ prepared by conventional precipitation, indicating the presence of active sites of higher strength on the CeO₂ prepared by microwave-assisted heating.

(c) Interaction with Methanol. Interaction with methanol was studied both on the two CeO₂ samples prepared by precipitation and on the one obtained by microwave-assisted heating to evaluate the effect of the synthesis, the thermal treatment, the surface chemical composition [presence of Ce(IV) and/or Ce(III)], the specific surface area, and the particle sizes on the surface reactivity. The IR data concerning liquid- and gas-phase methanol as well as some methoxy species adsorbed on unreduced and reduced ceria are reported in Table 3.

(i) CeO₂ (523 K). The DRIFT spectra collected after the exposure of the CeO₂ powder to methanol + N₂ at different temperatures are shown in Figure 11a–c. Gas phase and molecularly chemisorbed methanol dominates the C–O

(54) Falk, M.; Whalley, E. *J. Chem. Phys.* **1961**, *34*, 1554.

(55) Herzberg, G. *Infrared and Raman Spectra of Polyatomic Molecules*; Van Nostrand: New York, 1949.

(56) Badri, A.; Binet C.; Lavalley, J.-C. *J. Chem. Soc., Faraday Trans.* **1997**, *93*, 1159.

(57) Binet, C.; Jadi, A.; Lavalley, J.-C. *J. Chim. Phys.* **1992**, *89*, 1441.

(58) Binet, C.; Daturi, M. *Catal. Today* **2001**, *70*, 155.

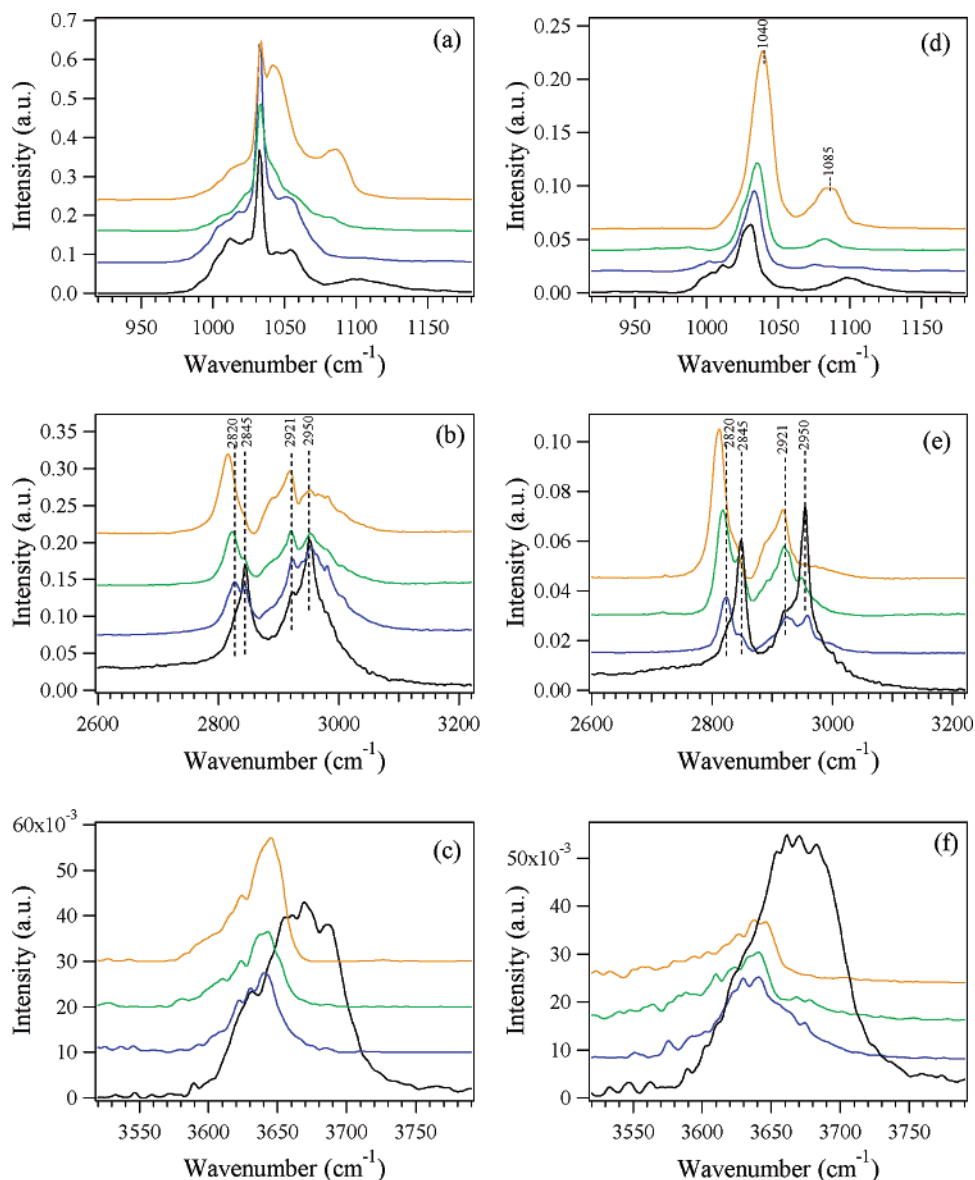


Figure 11. DRIFT spectra obtained after exposure of the CeO₂ powder obtained by precipitation and calcination at 523 K to methanol + N₂ mixture (a–c) and successively to N₂ flow (d–f) at different temperatures: (black RT, (blue 373 K, (green) 423 K, and (orange) 473 K: (a, d) C–O stretching region; (b, e) C–H stretching region; (c, f) O–H stretching region.

(peaks at 1012, 1032, and 1054 cm⁻¹) and the C–H (peaks at 2845 and 2950 cm⁻¹) stretching regions (Figure 11a,b and Table 3). At RT a weak band around 1100 cm⁻¹ suggests a certain dissociative interaction, which is slightly more evident when the excess of gas-phase methanol is outgassed. Figure 11d–f shows the DRIFT spectra obtained after the exposure to methanol + N₂ and successively to N₂. The inspection of the C–O stretching region (Figure 11d) allows us to individuate several contribution around 1020, 1030, 1056, and 1100 cm⁻¹. The comparison with the literature data (Table 3) suggests the formation of methoxy species tricoordinated [OCH₃(III), 1020 and 1030 cm⁻¹], bicoordinated [OCH₃(II), 1056 cm⁻¹], and monocoordinated [OCH₃(I), 1100 cm⁻¹] to Ce(IV). The presence of these species is also confirmed by the contributions at 2820 and 2921 cm⁻¹ attributed to symmetric and asymmetric C–H stretching of methoxy species (Figure 11e). The most intense band around 1030 cm⁻¹ is also due to molecularly chemisorbed methanol, whose presence is confirmed by the corresponding symmetric

and asymmetric C–H stretching contributions at 2845 and 2950 cm⁻¹ (Figure 11d,e).

Direct dissociation is preferred as suggested by the presence in the O–H stretching region of a broad band around 3580–3760 cm⁻¹ (Figure 11c,f). This band is constituted by several contributions at 3630, 3655, 3670, and 3687 cm⁻¹. The two signals at lower wavenumber can be ascribed to hydroxyl species bicoordinated to Ce(IV) cations, while those at higher wavenumber suggest the presence of hydroxyl species bicoordinated to reduced cations.⁴⁰

At $T \geq 373$ K, methanol dissociation is more favored. This phenomenon is particularly evident in the C–H stretching region (Figure 11b,e); in fact, at high temperature the contributions due to methoxy species (peaks at 2820 and 2921 cm⁻¹) become more and more evident, while those attributed to molecularly chemisorbed methanol (peaks at 2845 and 2950 cm⁻¹) decrease. Moreover it is noteworthy observing that the signals of methoxy species, besides increasing, shift from their initial positions. In the C–O

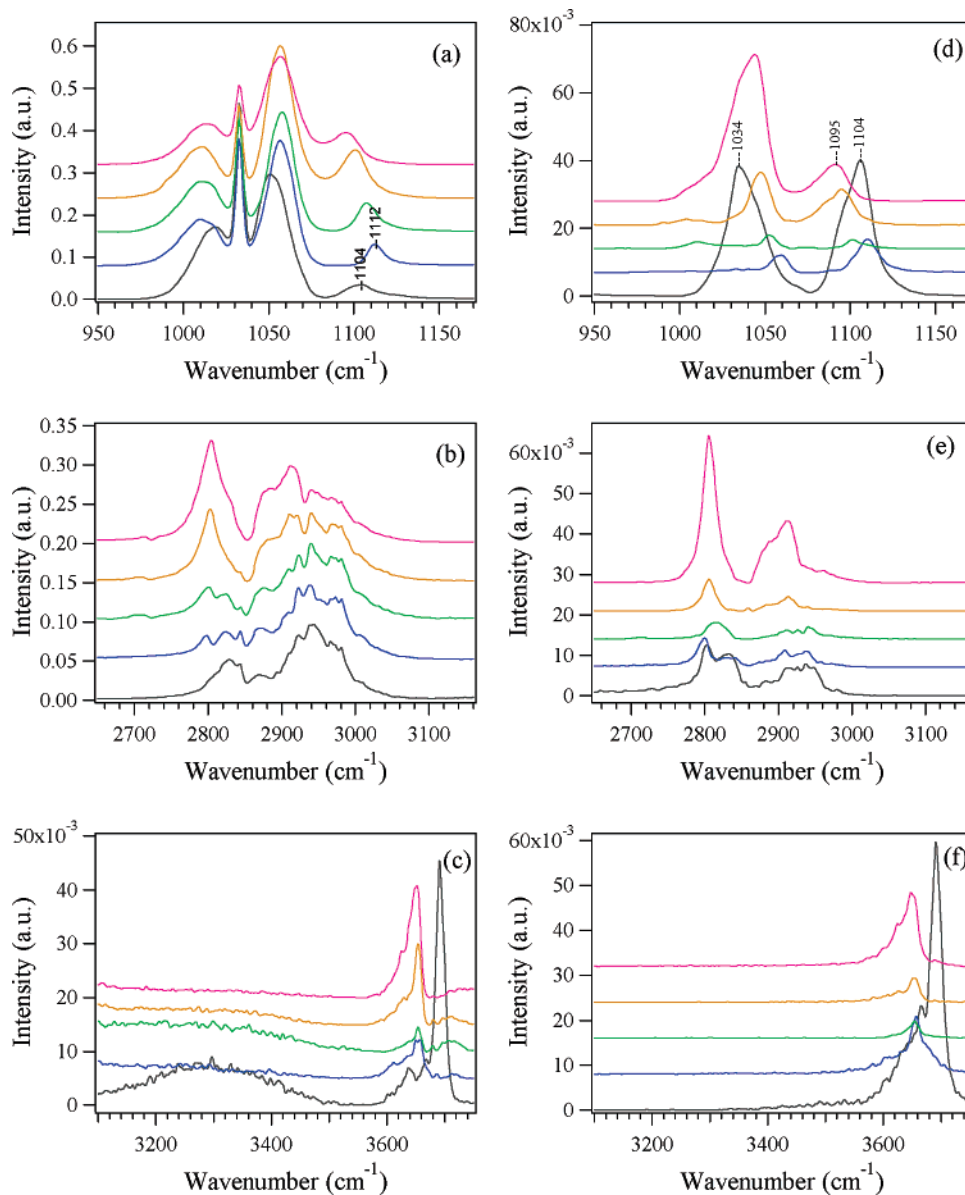


Figure 12. DRIFT spectra obtained after exposure of the CeO₂ powder obtained by precipitation and calcination at 923 K to methanol + N₂ mixture (a–c) and successively to N₂ flow (d–f) at different temperatures: (black) RT, (blue) 373 K (green) 423 K, (orange) 473 K, and (magenta) 523 K. (a, d) C–O stretching region; (b, e) C–H stretching region; (c, f) O–H stretching region.

stretching region (Figure 11a,d) the peaks attributed to tri- and bicoordinated methoxy groups (at 1030 and 1056 cm⁻¹) progressively shift toward higher wavenumber (at 1040 and 1085 cm⁻¹, respectively). These shifts are representative of a partial reduction of the CeO₂ surface. The effect of surface reduction is also clearly seen from the shift of symmetric stretching mode toward lower wavenumber (from 2820 to 2811 cm⁻¹).

Siokou and Nix⁵⁹ reported that the frequency shifts induced by surface reduction may be explained by considering the effect of varying the amount of negative charge localized on the oxygen of methoxy group. Simple valence bond representations indicate that as the negative charge localized on the oxygen increases [corresponding to a change in the oxidation state of metal atoms from Ce(IV) to Ce(III)], then the C–O bond order and its stretch frequency will increase while methyl group frequencies will decrease. These changes

confirm that methoxy groups can be a very useful tool for probing the structural and chemical nature of the oxide surface.

It is remarkable to note that from 373 K onward the peak at 1100 cm⁻¹, attributed to monocoordinated methoxy species, disappears, suggesting that these species are not stable at high temperature. However, the formation of a broad peak around 1080 cm⁻¹, which increases with temperature, could mean that the adsorption sites for monocoordinated methoxy species are converted into the ones corresponding to bicoordinated methoxy species upon reduced ceria.^{56,58}

N₂ does not completely remove the adsorbed species, not even at high temperature, suggesting a strong interaction with CeO₂ surface.

(ii) CeO₂ (923 K). Gas-phase and molecularly chemisorbed methanol also dominate the DRIFT spectra obtained after the exposure of the CeO₂ powder prepared by precipitation and calcined at 923 K to methanol + N₂ (Figure 12a–

(59) Siokou, A.; Nix, R. M. *J. Phys. Chem. B* **1999**, *103*, 6984.

c) at temperature ranging from RT to 573 K. A certain dissociative interaction can be more easily observed in the DRIFT spectra obtained after the exposure to methanol + N₂ and successively to N₂ (Figure 12d–f).

At RT two broad bands are evident in the C–O stretching spectral range (Figure 12d): the former centered at 1034 cm⁻¹, and the latter at 1104 cm⁻¹. Molecularly chemisorbed methanol is the main contribution to the band at lower wavenumber. This result is confirmed by the signals corresponding to the symmetric and asymmetric C–H stretching observed at 2832 and 2937 cm⁻¹ (Figure 12e). Considering the width and the asymmetry of the band centered at 1034 cm⁻¹, however, the presence of tri- and bicoordinated methoxy species cannot be excluded. The band at 1104 cm⁻¹ is ascribable to methoxy species monocoordinated to Ce(IV) cations.^{56–58} Consistently, in the C–H stretching spectral range (Figure 12e) the two shoulders at 2804 and 2911 cm⁻¹ are respectively assigned to the symmetric and asymmetric C–H stretching modes of monocoordinated methoxy species.⁵⁸ The broad tail toward higher wavenumber of the band centered at 1104 cm⁻¹ (Figure 12d) also suggests the presence of methoxy species monocoordinated to Ce(III) cations. Several signals at 3637, 3668, and 3691 cm⁻¹, attributed to the O–H stretching mode (Figure 12c,f), agree with a direct dissociation mechanism, causing the formation of hydroxyl and methoxy groups. The positions of these peaks are almost identical to those observed on the sample before the exposure to methanol. The small band between 3100 and 3500 cm⁻¹ observed in the spectrum recorded after methanol + N₂ exposure (Figure 12c) is due to molecularly adsorbed methanol. Likewise, CeO₂ treated at 523 K methanol dissociation is favored by temperature increment.

At 373 K in the C–O stretching region (Figure 12a) a widening toward higher wavenumber of the band centered at 1054 cm⁻¹ is observed. Also the band due to OCH₃(I) species is shifted upward to 1112 cm⁻¹. These discreet shifts from 1054 to 1060 cm⁻¹ and from 1104 to 1112 cm⁻¹ suggest that some Ce(IV) sites are reduced to Ce(III).

Beginning from $T > 373$ K, the OCH₃(I) band undergoes a continuous shift from 1112 to 1095 cm⁻¹ characteristic of methoxy species bicoordinated to Ce(III) cations (Figure 12a,d). The increment of the intensity and the progressive loss of resolution between neighboring bands at 1054 and 1095 cm⁻¹ could be due to a type I to type II* site conversion.⁵⁸ The same loss of resolution is observed between the band due to C–H stretching modes at 2911 and 2922 cm⁻¹.

At 373 K in the O–H stretching spectral range, only a weak band around 3654 cm⁻¹ is observed. With increasing temperature, this band becomes more and more intense: its position and downshift recalls the hydroxyl observed on the as-prepared CeO₂ treated at 923 K after heating at 373 K. It is worth observing that in this case N₂ removes almost completely the methoxy species with the exception of RT and high temperature (Figure 12d,e).

Unlike the unreduced CeO₂ sample, temperature increment also favors the methanol oxidation on the reduced CeO₂ sample. Weak peaks at 1549 and 1592 cm⁻¹, attributed to O–C–O asymmetric stretching of formate species, can be

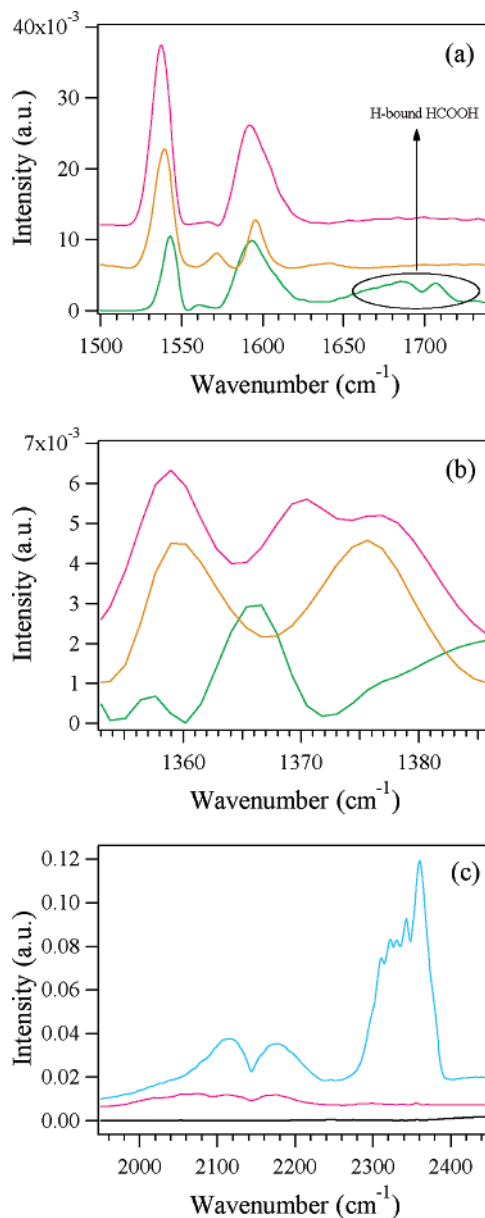


Figure 13. DRIFT spectra obtained after exposure of the CeO₂ powder obtained by precipitation and calcination at 923 K to methanol + N₂ at (green) 423 K, (orange) 473 K, (magenta) 523 K, and (pale blue) 573 K. (a) Region from 1500 to 1750 cm⁻¹; (b) region from 1353 to 1386 cm⁻¹; (c) region from 1950 to 2450 cm⁻¹.

observed upon exposure to methanol at $T \geq 423$ K (Figure 13a). Consistently, formate O–C–O symmetric stretching peaks (1359 and 1367 cm⁻¹) (Figure 13b) are evident.⁶⁰ With increasing temperature, the peaks of formate species become more evident. The peak positions (1359, 1367, 1549, and 1592 cm⁻¹) and shapes suggest the presence of mono- and bidentate formate species.^{59,60}

Formate is slightly bonded to the CeO₂ surface and can be easily removed from nitrogen flow. At 423 K, two weak peaks at 1685 and 1706 cm⁻¹ (Figure 13a) suggest the formation of the formic acid interacting by H-bond with the surface hydroxyl groups.⁶⁰

It is noteworthy to observe the formation of CO and CO₂ at 573 K (Figure 13c).

(60) Li, C.; Domen, K.; Maruya, K.; Onishi, T. *J. Catal.* **1990**, *125*, 445.

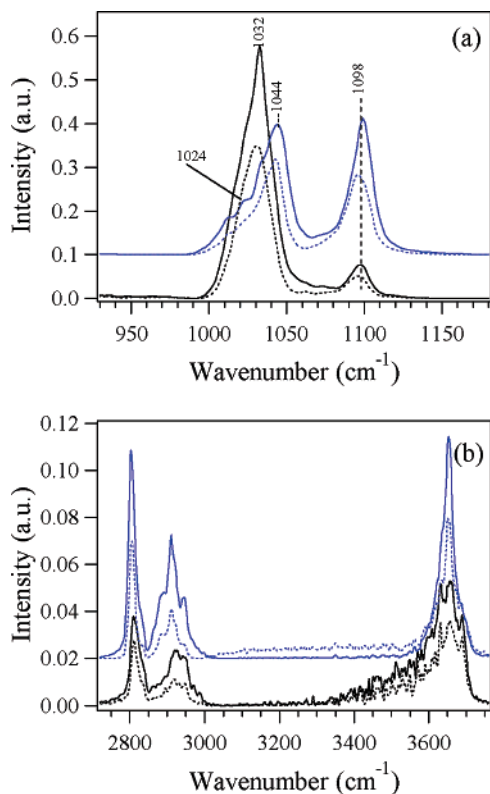


Figure 14. DRIFT spectra obtained after exposure of the CeO₂ obtained by microwave irradiation and calcination at 523 K to methanol + N₂ mixture (solid lines) and, successively, to N₂ flow (dotted lines) at different temperatures: (black) RT and (blue) 373 K. (a) C–O stretching region; (b) spectral region between 2720 and 3760 cm⁻¹.

(iii) **CeO₂(mw).** All the methanol introduced in the reaction chamber quantitatively reacts with the CeO₂ surface at RT (Figure 14, black solid line). Inspection of the C–O stretching region reveals the presence of two bands centered at 1032 and 1098 cm⁻¹, respectively (Figure 14a, black solid line). The wide and intense band centered at 1032 cm⁻¹ suggests that it is made up of several contributions: molecularly chemisorbed methanol and tri- and bicoordinated methoxy groups. Methoxy groups monocoordinated to Ce(IV) cations^{56–58} are mainly responsible for the band at 1098 cm⁻¹. The presence of methoxy groups is confirmed by the corresponding C–H symmetric and asymmetric stretching contributions at 2809, 2911, and 2920 cm⁻¹ (Figure 14b, black solid line).⁵⁸ Moreover, the weak intensity of the C–H stretching modes of molecularly chemisorbed methanol (shoulders at 2837 and 2945 cm⁻¹) suggests that the dissociation is more pronounced than the molecular interaction. This result is consistent with the major number of acidic/basic sites observed on this sample with respect to the ones prepared by precipitation.

The signals at 3631, 3658 and 3689 cm⁻¹ attributed to bicoordinated hydroxyl groups⁴⁰ agree with a direct dissociation mechanism (Figure 14b, black solid line). The formation of water molecules, revealed by the lower wavenumber tail around 3300–3550 cm⁻¹ and the corresponding hydroxyl bending peak at 1630 cm⁻¹, suggest also a condensation mechanism between methanol and hydroxyl groups.

At 373 K methanol dissociation is still more favored: all the peaks due to methoxy species increase. In the C–O

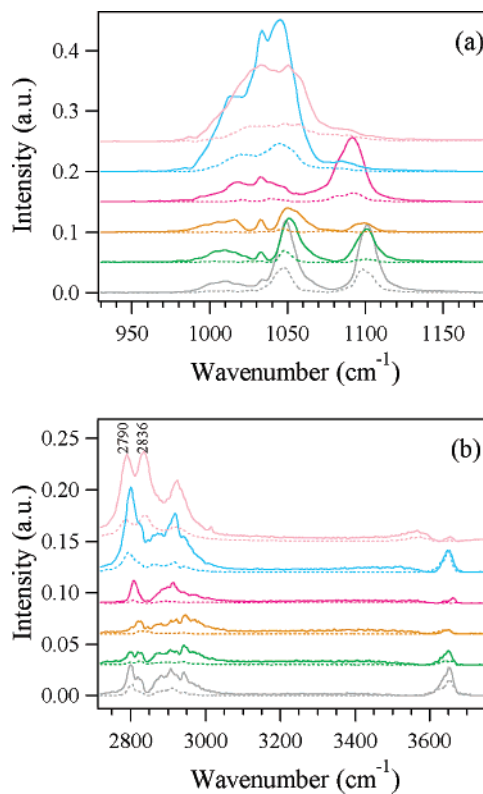


Figure 15. DRIFT spectra obtained after exposure of the CeO₂ obtained by microwave irradiation and calcination at 523 K to methanol + N₂ mixture (solid lines) and successively to N₂ flow (dotted lines) at different temperatures: (gray) 403 K, (green) 433 K, (orange) 473 K, (magenta) 523 K, (pale blue) 573 K, and (pale pink) 623 K. (a) C–O stretching region; (b) spectral region between 2720 and 3760 cm⁻¹.

stretching region (Figure 14a, blue solid line) the contributions of molecularly chemisorbed methanol disappear, while the contributions characteristic of tri- (shoulder at 1024 cm⁻¹) and bicoordinated (1044 cm⁻¹) methoxy groups become more and more evident. At this temperature direct dissociation is preferred, as suggested by the absence in the O–H stretching region of the tail due to molecularly chemisorbed water (Figure 14b, blue solid line).

N₂ does not significantly remove the adsorbed species from the sample surface at low temperature (Figure 14, dotted lines).

From 403 to 433 K methanol dissociation is less favored, and contributions due to gas-phase methanol are also evident in the spectra obtained after exposure to methanol + N₂ (Figure 15, solid lines).

At higher temperature new signals can be observed after exposure to methanol: between 1070 and 1115 cm⁻¹ (at 523 K) and 1045 cm⁻¹ (at $T \geq 573$ K) (Figure 15a, solid lines). The signals between 1070 and 1115 cm⁻¹ agree with the formation of methoxy species monocoordinated to Ce(IV) and Ce(III) cations. The peak at lower wavenumber (1045 cm⁻¹) is consistent with the presence of methoxy species tricoordinated to reduced cerium cations. This further reduction of sample surface is also confirmed from the shift of the C–H symmetric stretching contribution from 2809 to 2790 cm⁻¹ (Figure 15b, solid lines).

At higher temperature N₂ removes almost completely the methoxy species, suggesting a very weak interaction (Figure 15, dotted lines).

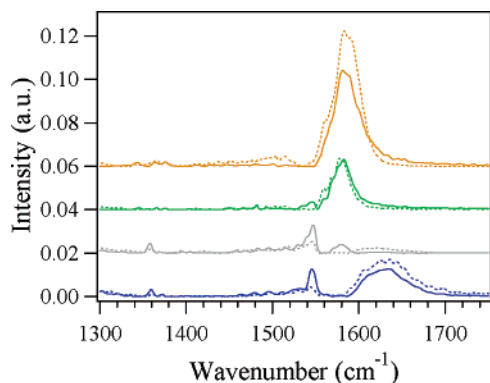


Figure 16. DRIFT spectra obtained after exposure of the CeO₂ obtained by microwave irradiation and calcination at 523 K to methanol + N₂ mixture (solid lines) and successively to N₂ flow (dotted lines) at different temperatures: (blue) 373 K, (gray) 403 K, (green) 433 K, and (orange) 473 K. The spectral region between 1300 and 1750 cm⁻¹ is shown.

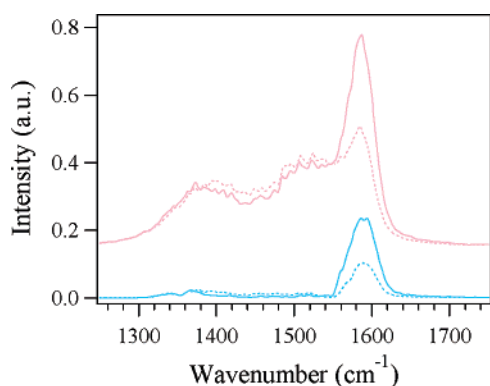


Figure 17. DRIFT spectra obtained after exposure of the CeO₂ obtained by microwave irradiation and calcination at 523 K to methanol + N₂ mixture (solid lines) and successively to N₂ flow (dotted lines) at (pale blue) 573 K and (pale pink) 623 K. The spectral region between 1250 and 1750 cm⁻¹ is shown.

At low temperatures this system shows a strong oxidizing capability. Formate species form after exposure at 373 K as suggested from the peaks at 1359, 1547, and 1581 cm⁻¹ (Figure 16, solid lines).^{59,60} The methanol oxidation is more favored at high temperature. A new contribution at 2836 cm⁻¹ (Figure 15b) is attributed to the C–H stretching of formate species. Also inorganic carboxylate (1509 cm⁻¹)⁴⁷ forms at 623 K (Figure 17, pale pink solid line). The nitrogen flow is not enough to remove the oxidation products from the surface (Figures 16 and 17, dotted lines).

Summarizing, the increment of the specific surface area and the higher presence of active sites (as suggested by the interaction with pyridine and carbon dioxide) can explain the higher reactivity in methanol dissociation of the CeO₂ obtained by microwave irradiation. Moreover, these results suggest that the presence of Ce(III) cations and the particle sizes are the key factors for methanol oxidation. In fact, the CeO₂ prepared by precipitation and treated at 523 K does not show any tendency to oxidize methanol, while the sample prepared by precipitation but characterized by a higher reduction degree of the surface (sample heated at 923 K) and the CeO₂ prepared by microwave irradiation and slightly reduced both evidence a higher oxidation capability. It is worth considering that the CeO₂ oxidation capability increases as size gets smaller.

Conclusions

Nanostructured CeO₂ powder was synthesized by two different procedures: precipitation from a basic solution and microwave-assisted heating hydrolysis. The two samples prepared with the first method were treated at two different temperatures, 523 and 923 K, respectively. The CeO₂ obtained by microwave irradiation was calcined at 523 K. At this temperature all the polymer used as a disperser stabilizer is removed.

XRD patterns are consistent with the presence of cubic CeO₂.

The analysis of TEM images reveals (i) a broad particle size distribution for the powders obtained by precipitation (average diameter is around 8.0–10.0 nm for CeO₂ treated at 523 K and around 12.0–15.0 nm for the one treated at 923 K) and (ii) small particles (average diameter is around 3.3–4.0 nm) with a narrow particle size distribution for the sample prepared by microwave irradiation and treated at 523 K.

XP outcomes show that the CeO₂ prepared by microwave-assisted heating is slightly reduced on the surface in comparison to the analogous one prepared by precipitation, but less reduced than the sample treated at 923 K. This different reduction degree is confirmed also by DRIFT results, which evidence the presence of hydroxyl groups coordinated to Ce(III) cations on the surface of the CeO₂ treated at 923 K.

In general, the samples prepared by precipitation show a lower specific surface area than the one obtained by microwave irradiation. Moreover, with the increment of heating temperature, the specific surface area decreases. The CeO₂ prepared by microwave-assisted heating is microporous powder, while the two CeO₂ samples prepared by precipitation are mesoporous powders.

The exposure to pyridine indicates the presence of Lewis and Brønsted acidic sites on the CeO₂ prepared by precipitation and treated at 923 K and even more on the CeO₂ obtained by microwave irradiation. It is interesting that pyridine interacting with the sample surface favors the release of free hydroxyl groups bicoordinated to Ce(IV) cations on the CeO₂ obtained by microwave-assisted heating, to Ce(III) cations on the sample prepared by precipitation and heated at 923 K. H-bound pyridine is the only species, beyond the liquidlike, revealed on the CeO₂ prepared by precipitation and heated at 523 K.

The exposure to CO₂ allows us to recognize the presence of basic sites and of complex sites constituted by a Lewis acidic site and a coordinatively unsaturated neighboring oxygen anion on the two samples characterized by a reduced surface. CO₂ does not interact with the surface of the sample prepared by precipitation and treated at 523 K, because the active sites distributed on the surface have already reacted with the atmospheric carbon dioxide.

Methanol interacts mainly dissociatively with the CeO₂ surface regardless of the preparation procedure and reduction degree of the surface. However, otherwise from the samples obtained by precipitation, on the CeO₂ prepared by microwave irradiation all the introduced methanol quantitatively reacts with the surface at RT.

The CeO₂ obtained by precipitation and treated at 523 K does not oxidize methanol, even at higher temperature, while a weak oxidation capability is noted on the sample slightly reduced (treated at 923 K). Methanol oxidation is more favored on the CeO₂ prepared by microwave irradiation. Formate species are observed at rather low temperatures (373 K) and increase with temperature. At higher temperature, inorganic carboxylate is also observed.

Acknowledgment. We gratefully acknowledge Professor E. Tondello for his helpful discussions, Dr. R. Saini for thermal analysis, and Professor R. Camprostrini and Dr. Marco Ischia for the BET measurements. This work was supported by research program FISR-MIUR, Nanosistemi inorganici ed ibridi per lo sviluppo e l'innovazione di celle a combustibile.

CM051352D